# Local vibrational modes of the metastable dicarbon center ($C_s$–$C_i$) in silicon

E. V. Lavrov, L. Hoffmann, and B. Bech Nielsen
*Institute of Physics and Astronomy, University of Aarhus, DK-8000 Aarhus C, Denmark*
(Received 6 January 1999)

The metastable dicarbon center ($C_s$–$C_i$) in silicon has been studied by infrared absorption spectroscopy. After electron irradiation of carbon-doped silicon, new infrared absorption lines at 540.4, 543.3, 579.8, 640.6, 730.4, and 842.4 $cm^{-1}$ are observed. The lines are identified as local vibrational modes of the $C_s$–$C_i$ center in its $\mathcal{B}$ form. Illumination of the sample with band-gap light at ~60 K converts the $\mathcal{B}$ to the $\mathcal{A}$ form, and local modes of the $\mathcal{A}$ form are identified at 594.6, 596.9, 722.4, 872.6, and 953 $cm^{-1}$. The observed local mode frequencies of both forms are in excellent agreement with those calculated from *ab initio* theory. Our findings provide strong support for the atomic structure suggested previously for the two forms. [S0163-1829(99)07635-3]

## I. INTRODUCTION

In crystalline silicon, carbon atoms are common and important impurities which are predominantly located at substitutional sites.[1] Interstitial carbon, $C_i$, is formed when mobile silicon interstitials, produced by electron irradiation, are trapped by substitutional carbon, $C_s$.[1–3] At room temperature, $C_i$ migrates through the lattice and becomes trapped at $C_s$, whereby a dicarbon center, $C_s$–$C_i$, is formed.[4] This center has been investigated extensively,[1,4–15] and its characteristic spectroscopic signatures were known for a number of years before the atomic structure of the center was identified. $C_s$–$C_i$ was studied by photoluminescence,[5] electron paramagnetic resonance (EPR),[4,6] infrared absorption spectroscopy,[7] photoconductivity,[8] deep-level transition spectroscopy (DLTS),[9,10] and optically detected magnetic resonance (ODMR).[11] It was established that the center is metastable and can exist in two configurations, labeled the $\mathcal{A}$ form and the $\mathcal{B}$ form. The point group of the $\mathcal{A}$ form is $C_{1h}$, and it represents the global minimum in energy for the singly positive and singly negative charge states, $\mathcal{A}^{\pm}$. The atomic model deduced from EPR and DLTS experiments consists of a $\langle 100 \rangle$-oriented Si–C split-interstitial adjacent to a second substitutional carbon atom.[10] The $\mathcal{B}$ form is energetically favored in the neutral charge state, and it also has a $C_{1h}$ point group.[1] The proposed atomic structure of this form consists of two equivalent substitutional carbon atoms at neighboring lattice sites with an interstitial silicon atom located between them.[10] Recent *ab initio* calculations qualitatively confirmed these atomic structures of the $\mathcal{A}$ and $\mathcal{B}$ forms of $C_s$–$C_i$.[13–15]

Knowledge about local vibrational modes (LVM's) gives detailed insight into the physical properties of light atoms embedded in silicon. The LVM's reveal rather directly which chemical bonds the light atoms form with their neighbors. Hence, the frequencies of the LVM's depend critically on the atomic structure of the light-atom defect. Information about LVM's of $C_s$–$C_i$ was previously obtained from photoluminescence studies. The $\mathcal{B}$ form gives rise to a zero-phonon luminescence line, the so-called $G$ line, at 969 meV.[1] Phonon-assisted transitions associated with this line revealed three LVM's at 543.3, 579.8, and 730.4 $cm^{-1}$ (see Refs. 1 and 12). However, six LVM's in total should be expected for $C_s$–$C_i$, corresponding to the six degrees of freedom of the two carbon atoms. Moreover, no LVM of the $\mathcal{A}$ form has been identified so far.

In this paper the LVM's of the $\mathcal{A}$ and $\mathcal{B}$ forms are established by infrared (IR) absorption spectroscopy. The observed LVM's are in excellent agreement with those calculated from *ab initio* theory.[13–15] Thus, the present work provides additional support to the structures of $C_s$–$C_i$ proposed previously.

## II. EXPERIMENTAL DETAILS

Samples with dimension $\sim 10 \times 10 \times 2$ $mm^3$ were cut from two high-resistivity float-zone silicon crystals doped predominantly with $^{12}C$ (Si:$^{12}C$) or $^{13}C$ (Si:$^{13}C$). The samples were subsequently mechanically polished on the two opposite $10 \times 10$ $mm^2$ surfaces to ensure maximum transmission of infrared light. The concentrations of carbon and oxygen were estimated from the intensities measured at 10 K of the LVM's of $^{12}C_s$ (or $^{13}C_s$) at 607 $cm^{-1}$ (or 589 $cm^{-1}$) and of interstitial oxygen ($^{16}O$) at 1136 $cm^{-1}$ (see Ref. 16). The Si:$^{12}C$ crystal contained $4.5 \times 10^{17}$ $cm^{-3}$ $^{12}C$ and $\sim 1 \times 10^{16}$ $cm^{-3}$ $^{16}O$ atoms, whereas the Si:$^{13}C$ crystal contained $8.0 \times 10^{17}$ $cm^{-3}$ $^{13}C$, $\sim 1 \times 10^{17}$ $cm^{-3}$ $^{12}C$, and $\sim 1 \times 10^{17}$ $cm^{-3}$ $^{16}O$ atoms.

The samples were irradiated with 2.3 MeV electrons supplied by a 5 MeV Escher Holland van de Graaff accelerator. The electrons were mass analyzed by a magnet which deflected the beam into a 6-m-long beamline, forming an angle of ~15° with the exit beam from the accelerator. During the irradiation, the samples were mounted inside a vacuum chamber on a copper block, which was in good thermal contact with the cold finger of a closed-cycle helium cryocooler. At the beginning of the irradiation, the temperature on the copper block was 70 K. The total irradiation dose was $\sim 10^{18}$ $cm^{-2}$, and the current density was kept below $2 \times 10^{13}$ $cm^{-2}$ $s^{-1}$ to ensure that the temperature on the block did not exceed 200 K. The background pressure in the vacuum chamber was below $10^{-4}$ torr.

After the irradiation, the samples were stored in liquid nitrogen for up to 70 h, before they were mounted in a

 

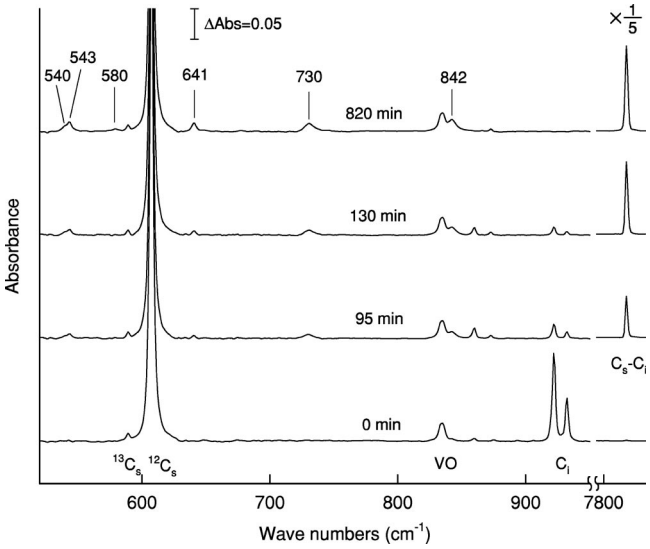


FIG. 1. Sections of absorbance spectra of electron-irradiated Si:$^{12}$C recorded at 10 K just after irradiation and after subsequent heat treatment at room temperature for 95, 130, and 820 min.

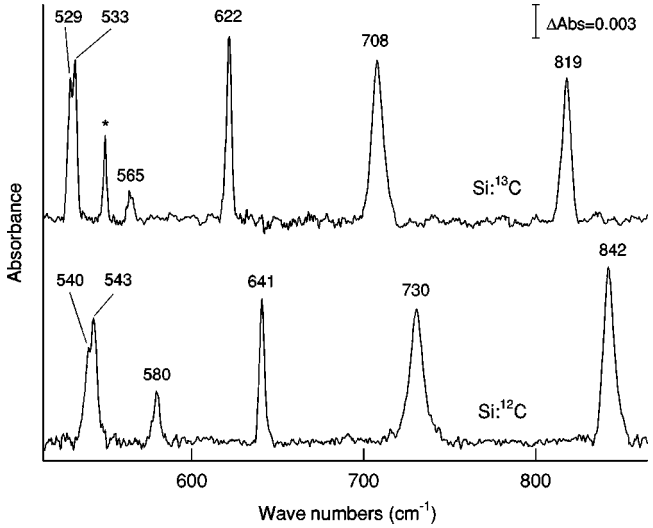


FIG. 2. Section of absorbance spectra of electron-irradiated Si:$^{12}$C and Si:$^{13}$C recorded at 10 K after heat treatment at room temperature for 820 min and several days, respectively. The absorption line denoted by an ⋆ is not related to a carbon mode (see text).

closed-cycle helium cryostat designed for optical measurements. During the mounting process, the samples were allowed to warm up to room temperature for as short a time as possible (about 10 min). This procedure was employed to reduce the diffusion of the $C_i$'s created by the irradiation.

The IR absorbance spectra were recorded with a Nicolet, System 800, Fourier-transform spectrometer. The measurements were carried out with a Ge-on-KBr beamsplitter, a glowbar, or a tungsten lamp as light source, and a mercury cadmium telluride (MCT) detector. The spectra were recorded at 10 K with an apodizied resolution of 2 cm$^{-1}$, unless cited otherwise.

In order to study the thermal stability of the absorption lines, an IR spectrum was recorded at 10 K after each step in a series of isochronal heat treatments at temperatures in the range from room temperature to 300 °C. Each heat treatment had a duration of 30 min and was carried out in a nitrogen atmosphere. In each step, the temperature was increased by 20 ° C.

As described in Sec. III, the $\mathcal{A}$ form of $C_s$–$C_i$ may be produced from the $\mathcal{B}$ form by photoexcitation, i.e., illumination with band-gap light. The photoexcitation was performed with the tungsten lamp mounted in the spectrometer.

## III. RESULTS

### A. LVM's of the $\mathcal{B}$ form of $C_s$–$C_i^0$

Figure 1 shows the IR absorbance spectra of the electron-irradiated Si:$^{12}$C, recorded just after the irradiation and after subsequent heat treatments at room temperature for 95, 130, and 820 min. From all the spectra, a reference spectrum has been subtracted, recorded on pure silicon with a low carbon content. The most intense absorption line in the spectra located at 607 cm$^{-1}$ represents the LVM of $^{12}C_s$. The dominant defect produced in carbon-doped silicon by electron irradiation below room temperature is $C_i$, which possesses two IR-active modes at 922 and 932 cm$^{-1}$. As can be seen from the figure, both modes are observed just after the irradiation in agreement with previous reports.[2] At about room temperature, $C_i$ becomes mobile and is trapped by residual $C_s$, whereby $C_s$–$C_i$ is formed. It is evident from Fig. 1 that the intensities of the LVM's of $C_i$ decrease as a function of heating time at room temperature, and after 820 min the $C_i$ modes can no longer be detected. The concurrent formation of $C_s$–$C_i$ can be monitored via the IR absorption line at 7819 cm$^{-1}$. This electronic transition corresponds to the formation of an electron-hole pair bound to the $\mathcal{B}$ configuration of $C_s$–$C_i$.[7] The reverse process, i.e., the recombination of the electron-hole pair, gives rise to the *G* line observed at 7819 cm$^{-1}$ in photoluminescence.[5] The growth of the 7819-cm$^{-1}$ line as a function of heating time is clearly seen from the figure. Hence, $C_s$–$C_i$ is formed in our samples.

In addition to the 7819-cm$^{-1}$ line, six new absorption lines in the range from 500 to 900 cm$^{-1}$ grow during the heat treatment at room temperature. The intensities of the new lines at 540.4, 543.3, 579.8, 640.6, 730.4, and 842.4 cm$^{-1}$ are low compared with the intensity of the $^{12}C_s$ line at 607 cm$^{-1}$, even after 820 min at room temperature. Fortunately, a 30-min heat treatment at 270 °C removes the six new lines from the spectrum without causing significant changes in the intensities of the multiphonon absorption bands and of the other lines, including the $^{12}C_s$ line at 607 cm$^{-1}$ and the vacancy-oxygen (VO or *A* center) line at 836 cm$^{-1}$.[17] Therefore, the spectra recorded after heat treatment at 270 °C have been used as reference spectra to remove the intense spectral features which dominate and obliterate the lines of interest. The spectra shown in Fig. 2 were obtained this way. As can be seen from the figure, the frequencies of the six lines shift downwards when $^{12}$C is substituted by $^{13}$C. The average ratio between the frequencies of the corresponding lines in the Si:$^{12}$C and Si:$^{13}$C spectra is 1.027. For a carbon atom bound to a silicon atom by a harmonic spring, the corresponding ratio is $\sqrt{m_r^{13}/m_r^{12}}=1.028$, where $m_r^{12}$ and $m_r^{13}$ are the reduced masses of Si–$^{12}$C and Si–$^{13}$C. Therefore, we ascribe the six absorption lines to LVM's of a carbon defect. We note that an additional line is

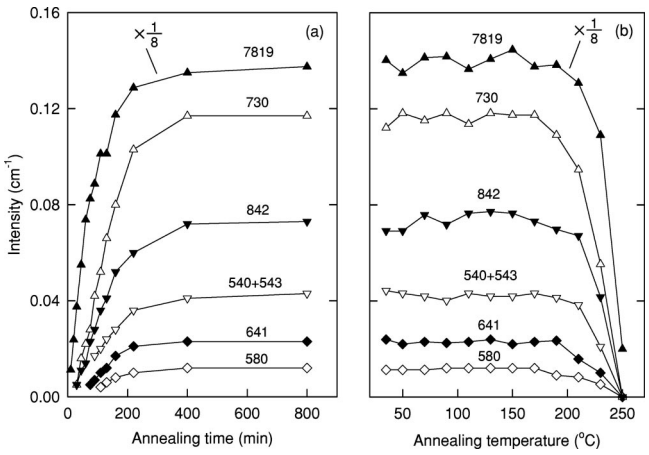


FIG. 3. The intensity (integrated absorbance) of the 7819-$cm^{-1}$ (▲), 730-$cm^{-1}$ (△), 842-$cm^{-1}$ (▼), (540 +543)-$cm^{-1}$ (▽), 641-$cm^{-1}$ (◆), and 580–$cm^{-1}$ (◇) lines measured at 10 K on electron-irradiated Si:$^{12}$C: (a) after successive heat treatments at room temperature and (b) after each step in a series of isochronal heat treatments for 30 min in a nitrogen atmosphere. The intensity of the 7819-$cm^{-1}$ line has been scaled down by a factor of 8.

observed at $\sim 550$ $cm^{-1}$ in the Si:$^{13}$C spectrum. This line is observed also in Czochralski-grown silicon doped with $^{12}$C. Thus, it does not represent an LVM of a carbon defect.

In Fig. 3, the formation and annealing behaviors of the 7819-$cm^{-1}$ line and the six new LVM's are compared. From the figure, it is clear that the LVM's and the 7819-$cm^{-1}$ line appear and disappear simultaneously. This strongly suggests that the six LVM's originate from $C_s$–$C_i$. Moreover, the modes at 543.3, 579.8, and 730.4 $cm^{-1}$ coincide with those previously assigned to the $\mathcal{B}$ form of $C_s$–$C_i$ in its neutral charge state on the basis of photoluminescence measurements.[1,12] We therefore conclude that the LVM's at 540.4, 543.3, 579.8, 640.6, 730.4, and 842.4 $cm^{-1}$ originate from the $\mathcal{B}$ configuration of $C_s$–$C_i^0$.

### B. LVMs of the $\mathcal{A}$ form of $C_s$–$C_i^0$

It is not surprising that no IR signatures of the $\mathcal{A}$ form are seen in the spectra shown in Fig. 2. The starting materials have high resistivities, and irradiation with electrons at doses above $10^{18}$ $cm^{-2}$ forces the Fermi level into the middle of the band gap. The $\mathcal{A}$ configuration has a donor $(0/+)$ and an acceptor $(-/0)$ level located at $E_v+90$ meV and $E_c-170$ meV, respectively.[9,10] This implies that $C_s$–$C_i$ is produced in the neutral charge state, where the $\mathcal{B}$ form is the minimum-energy configuration. The limited sensitivity of IR spectroscopy prevents us from working with much lower irradiation doses, and hence we cannot raise or lower the Fermi level enough to observe the $\mathcal{A}$ form directly by reducing the dose. However, it is possible to convert the $\mathcal{B}$ form to the $\mathcal{A}$ form by photoexcitation of the sample with band-gap light. During the illumination, some of the centers capture photoinduced electrons or holes, whereby the $\mathcal{A}$ form becomes energetically favorable. The conversion reactions between the $\mathcal{A}$ and the $\mathcal{B}$ forms have been studied in detail by EPR and DLTS.[9,10] The most interesting reactions are $\mathcal{B}^+ \rightarrow \mathcal{A}^+$ and $\mathcal{B}^- \rightarrow \mathcal{A}^-$. Of these two, the process $\mathcal{B}^+ \rightarrow \mathcal{A}^+$ may be disregarded since it is much slower than $\mathcal{B}^- \rightarrow \mathcal{A}^-$ (Ref. 10). The time constant of the latter thermally activated reaction is[10]

$$\tau_{\mathcal{B}\rightarrow\mathcal{A}} = 6.4\times 10^{-13}\ \text{sec}\times \exp(0.15\ \text{eV}/kT),$$

whereas the process going back, $\mathcal{A}^- \rightarrow \mathcal{B}^-$, has a characteristic time[10]

$$\tau_{\mathcal{A}\rightarrow\mathcal{B}} = 7.5\times 10^{-13}\ \text{sec}\times \exp(0.174\ \text{eV}/kT).$$

Hence, $\tau_{\mathcal{B}\rightarrow\mathcal{A}}$ is less than $\tau_{\mathcal{A}\rightarrow\mathcal{B}}$ at all temperatures, which implies that the $\mathcal{B}$ form can be partly converted into the $\mathcal{A}$ form by photoexcitation. It is important that the time needed to cool the sample ($\sim 10$ min) from the temperature of illumination to the temperature, where the process $\mathcal{A}^- \rightarrow \mathcal{B}^-$ freezes in, is much less than $\tau_{\mathcal{A}\rightarrow\mathcal{B}}$. Otherwise, the system will go back to the $\mathcal{B}$ form during cooling. On the other hand, $\tau_{\mathcal{B}\rightarrow\mathcal{A}}$ should be smaller than the illumination time, which as a matter of convenience we choose to be 20 min. If we require that $\tau_{\mathcal{B}\rightarrow\mathcal{A}} \leqslant 20\ \text{min} \leqslant \tau_{\mathcal{A}\rightarrow\mathcal{B}}$, the illumination should be carried out in the narrow temperature interval from 50 to 60 K to comply with these conditions.

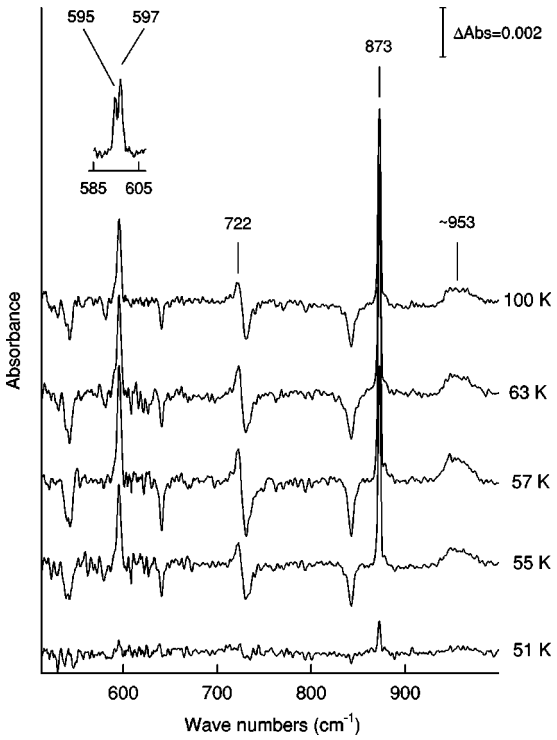


FIG. 4. Section of absorbance spectra recorded at 10 K on electron-irradiated Si:$^{12}$C after illumination with band-gap light at different temperatures in the range 51–100 K. All spectra have been subtracted by the spectrum measured directly after cooling from room temperature to 10 K in darkness. The inset shows a small part of the spectrum recorded with resolution 1 $cm^{-1}$ at 10 K after illumination at 57 K.

The IR spectra recorded at 10 K on Si:$^{12}$C after 20-min illumination at different temperatures in the range 50–100 K are presented in Fig. 4. In each case, the illumination was continued during the cooling of the sample, until the temperature came below 30 K. The spectra in the figure have been subtracted by the spectrum measured on the same sample at 10 K after cooling from room temperature with no

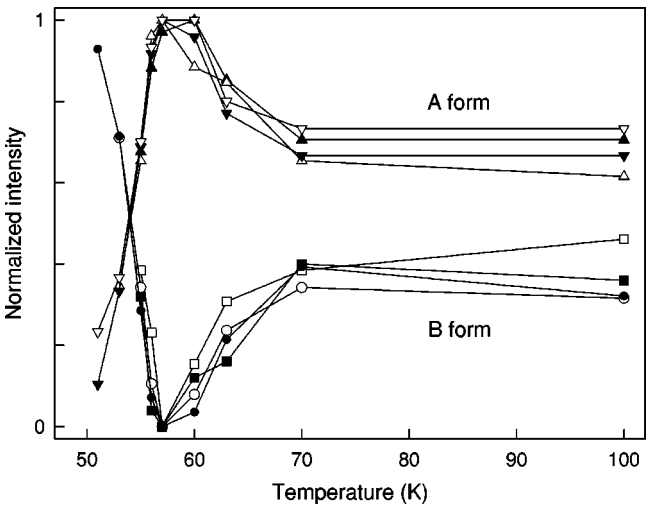


FIG. 5. Normalized intensities of the IR absorption peaks associated with the $\mathcal{A}$ and the $\mathcal{B}$ configurations of $C_s$–$C_i$ shown as a function of illumination temperature. The intensities have been normalized to their maximum value (the $\mathcal{A}$ form) or to their maximum change (the $\mathcal{B}$ form). The illumination time at each temperature was 20 min. After the illumination, the sample was cooled down to 10 K where the IR spectra were measured. (▲) 594.6 +596.9 $cm^{-1}$; (△) 722.4 $cm^{-1}$; (▼) 872.6 $cm^{-1}$; (▽) 953 $cm^{-1}$; (■) 540.4+543.3 $cm^{-1}$; (□) 640.6 $cm^{-1}$; (●) 730.4 $cm^{-1}$; (○) 842.4 $cm^{-1}$.

illumination of the sample. As can be seen from the figure, illumination at temperatures above 50 K gives rise to new absorption lines at 594.6, 596.9, 722.4, 872.6, and 953 $cm^{-1}$. When $^{12}C$ is substituted by $^{13}C$, these lines shift downwards in frequency, which demonstrates that they represent LVM's of carbon. Furthermore, the growth of the illumination-induced LVM's occurs parallel with the decrease of the LVM's of the $\mathcal{B}$ form, which are revealed as dips in Fig. 4. The maximum change in the intensities of both sets of modes, i.e., the maximum peaks and dips in the figure, were observed after illumination at 57 K. At this temperature, the intensities of the LVM's of the $\mathcal{B}$ form in the raw spectrum decreased by 20% as a result of the illumination. In Fig. 5, the intensities of the illumination-induced LVM's, normalized to their maximum values, are shown against the illumination temperature. In addition, the decrease in the intensities of the $\mathcal{B}$ form LVM's, normalized to their maximum drop (20%), is also shown. From the figure, it is evident that the two sets of LVM's are anticorrelated. This finding suggests that the two sets of carbon LVM's are associated with different configurations of the same defect. Moreover, the illumination-induced LVM's can be removed, and the LVM's of the $\mathcal{B}$ form can be fully recovered by a heat treatment at 60 K or above in darkness. Finally, the highest intensities of the illumination-induced LVM's are obtained within the narrow temperature interval, where the partial conversion of the $\mathcal{B}$ form to the $\mathcal{A}$ form should proceed most efficiently. On this basis, we conclude that the illumination-induced LVM's originate from the $\mathcal{A}$ form of $C_s$–$C_i$. The charge state of the center cannot be established directly from our measurements alone. However, with a Fermi-level position close to midgap, the singly positive and singly negative charge states of $C_s$–$C_i$ are unstable. Hence, $\mathcal{A}^{\pm}$ should relax to $\mathcal{A}^0$ when the illumination is switched off.

## IV. DISCUSSION

### A. Comparison with theory

In Table I, the observed LVM frequencies of the $\mathcal{B}$ form are compared with those calculated by Leary *et al.*[13,14] and Capaz *et al.*,[15] using *ab initio* theory. As mentioned above, the LVM's at 543.3, 579.8, and 730.4 $cm^{-1}$ were observed previously by photoluminescence. Moreover, in the photoluminescence spectra, a weak phonon replica line is resolved, which corresponds to the 842.4-$cm^{-1}$ mode.[1] Presumably, the low intensity of this line did not allow the authors to identify it as an LVM of the $\mathcal{B}$ form. Only modes transforming like the totally symmetric irreducible representation *A* can be observed by photoluminescence. A simple analysis based on group theory shows that the $\mathcal{B}$ form should possess four *A* modes and two *B* modes. Thus, the photoluminescence data suggest that the LVM's at 540.4 and 640.6 $cm^{-1}$ are *B* modes, whereas the remaining four modes are *A* modes. This constitutes the experimental basis for the identification of the symmetry properties in Table I. For all *A* modes, the motions of the two carbon atoms are restricted to the mirror plane, whereas for the *B* modes, the carbon atoms move perpendicular to this plane.

As can be seen from the table, the observed and calculated frequencies agree very well. The frequencies calculated by Leary *et al.*[13,14] deviate at most by 16 $cm^{-1}$ from those observed, whereas the values given by Capaz *et al.*[15] deviate a bit more for the two LVM's with lowest frequencies. The only discrepancy between observed and calculated LVM's is the ordering of the two modes (*A* and *B*) with the lowest frequencies. The experiment shows that the *B* mode has the

TABLE I. Experimental and calculated LVM frequencies ($cm^{-1}$) of $C_s$–$C_i$ ($\mathcal{B}$ form).

| Symm. | $^{12}C$–$^{12}C$ | | | $^{13}C$–$^{13}C$ | | |
|---|---|---|---|---|---|---|
| | Expt. | Calc. (Ref. 13) | Calc. (Ref. 15) | Expt. | Calc. (Ref. 13) | Calc. (Ref. 15) |
| *A* | 842.4 | 837.9 | 841.1 | 818.5 | 815.8 | 819.3 |
| *A* | 730.4[a] | 714.8 | 715.7 | 707.7[a] | 691.7 | 690.7 |
| *B* | 640.6 | 648.7 | 643.4 | 621.8 | 630.3 | 624.1 |
| *A* | 579.8[a] | 582.3 | 567.0 | 564.6[a] | 568.2 | 551.3 |
| *A* | 543.3[a] | 543.2 | 502.8 | 532.9[a] | 538.5 | 499.0 |
| *B* | 540.4 | 551.8 | 513.8 | 529.3 | 543.0 | 506.4 |

[a]Modes also observed in PL.

TABLE II. Experimental and calculated LVM frequencies ($cm^{-1}$) of $C_s$–$C_i$ ($\mathcal{A}$ form).

| Symm. | $^{12}C$–$^{12}C$ | | | $^{13}C$-$^{13}C$ | | |
|---|---|---|---|---|---|---|
| | Expt. | Calc. (Ref. 14) | Calc. (Ref. 15) | Expt. | Calc. (Ref. 14) | Calc. (Ref. 15) |
| *A* | 953 | 987.6 | 889.9 | | 960.1 | 862.5 |
| *B* | 872.6 | 776.9 | 874.1 | 845.4 | 752.2 | 847.2 |
| *A* | 722.4 | 739.2 | 721.8 | 700.6 | 716.0 | 700.3 |
| *A* | 596.9 | 600.0 | 567.5 | 579.9 | 583.8 | 550.4 |
| *B* | 594.6 | 598.7 | 557.1 | 577.7 | 582.6 | 540.9 |
| *A* | | 531.3 | 160 | | 531.3 | |

lowest frequency but the splitting between the two modes is only 2.9 $cm^{-1}$. Certainly, the error bars of the calculated frequencies significantly exceed this value.

In Table II, the observed and calculated[13–15] mode frequencies of the $\mathcal{A}$ configuration are given. Since no LVM's of the $\mathcal{A}$ form have been determined from photoluminescence measurements, we are unable to identify the four *A* and two *B* modes on the basis of experimental data. However, the *ab initio* frequencies fit the experimental values reasonably well, although the maximum deviation is about 100 $cm^{-1}$ in this case. For both sets of calculations, the maximum deviation corresponds to one of the two LVM's with highest frequencies. Also, the difference between the frequencies obtained by the two groups is large for these specific modes. The experimental excitation energies of the two high-frequency modes are 0.11 and 0.12 eV, and, hence, they are comparable to the activation barrier of 0.15 eV separating the neutral charge states of the $\mathcal{A}$ and $\mathcal{B}$ configurations. This suggests that anharmonic effects are important and that the calculated quasiharmonic frequencies are inaccurate for these modes. The fact that the 953-$cm^{-1}$ line is very broad indicates that anharmonic effects may play an important role, at least for these modes.

For the $\mathcal{A}$ form, only five modes are detected, although the defect should possess six modes. According to the calculations, the LVM with the lowest frequency is close to or falls below the Raman frequency in silicon at 524 $cm^{-1}$.[18] If so, we expect this mode to couple strongly with the lattice phonons and thereby to escape observation due to significant broadening. Alternatively, the mode may fall below the detection limit of our setup at $\sim$430 $cm^{-1}$.

### B. Intensities of LVM's

The concentration of $C_s$–$C_i$, denoted $N_{C_s-C_i}$, we can estimate from the intensity, *I*, of the 7819-$cm^{-1}$ line,[1] using the expression

$$I=\int \alpha(\sigma)d\sigma = 6.8\times 10^{-16}\ \text{cm}\times N_{C_s-C_i}.$$

Here, the absorption coefficient $\alpha$ and the wave number $\sigma$ are in $cm^{-1}$. From the spectrum recorded after 820-min heat treatment at room temperature (see Fig. 1), we find that $N_{C_s-C_i}\approx 4.5\times 10^{16}$ $cm^{-3}$. Two independent estimates of $N_{C_s-C_i}$ can be obtained from the LVM intensities of the $\mathcal{A}$ and the $\mathcal{B}$ form. These estimates rely on the microscopic models of the two configurations and the reported effective charges of $C_s$ and $C_i$.[19] As described below, the estimates based on the LVM's are in fair agreement with the value stated above, and thus they provide additional support for the atomic models of the $\mathcal{A}$ and $\mathcal{B}$ configurations.

According to the molecular model of the $\mathcal{A}$ form, one of the carbon atoms may be considered as a perturbed substitutional carbon $C_s$. The presence of the adjacent Si–C split interstitial lowers the symmetry to $C_{1h}$, but the local symmetry of the $C_s$ and its four silicon neighbors is close to $C_{3V}$. Hence, the threefold-degenerate $T_2$ mode of isolated $C_s$ at 607 $cm^{-1}$ splits into two nearly degenerate modes resembling an *E* mode and a nondegenerate mode resembling an $A_1$ mode. The LVM at 722.4 $cm^{-1}$ is the $A_1$-like mode, whereas the LVM's at 594.6 and 596.9 $cm^{-1}$ correspond to the *E* mode. The other carbon atom of the $\mathcal{A}$ configuration has a local structure very similar to interstitial carbon $C_i$. As mentioned in Sec. III, $C_i$ gives rise to two LVM's at 922 and 932 $cm^{-1}$. This suggests that the $\mathcal{A}$ form modes at 872.6 and 953 $cm^{-1}$ basically are the LVM's of $C_i$ perturbed by the neighboring $C_s$. Based on this qualitative picture, we suggest that the effective charges[20] associated with the two groups of LVM's are the same as for the isolated defects, i.e., $\eta_s=2.4e$ for $C_s$ and $\eta_i=3.2e$ for $C_i$.[19] If $\alpha_s(\sigma)$ and $\alpha_i(\sigma)$ denote the sum of the absorption coefficients of the $C_s$-like and the $C_i$-like LVM's, respectively, the concentration of IR active centers, *N*, can be estimated from

$$\int \alpha_x(\sigma)d\sigma=\frac{\pi\eta_x^2 N}{n_R c^2 M_{\text{imp}}},\quad x=s,i.$$

$n_R$ is the refractive index, *c* the velocity of light, and $M_{\text{imp}}$ the mass of the carbon atom.[21,22] The integrals of $\alpha_s(\sigma)$ and $\alpha_i(\sigma)$ have been determined from the spectrum obtained after 820-min heat treatment at room temperature and subsequent cooling to 10 K in darkness followed by photoexcitation at 57 K. Now, the concentration *N* can be determined from the formula above. However, only 20 $C_s$–$C_i$ centers have the $\mathcal{A}$ configuration under these conditions, and, therefore, $N_{C_s-C_i}\approx 5\times N$ can be calculated from *N*. From the intensities of the $C_s$-like modes, we obtain $N_{C_s-C_i}\approx 5\times 10^{16}$ $cm^{-3}$, whereas the $C_i$-like modes give $N_{C_s-C_i}\approx 3.8\times 10^{16}$ $cm^{-3}$. These values deviate less than 16% from the $4.5\times 10^{16}$ $cm^{-3}$ estimated from the intensity of the

7819-cm$^{-1}$ line. We consider this agreement to be very good, taking into account the crudeness of the estimates.

Because the two carbon atoms in the $\mathcal{B}$ configuration are fourfold coordinated and located near-substitutionally, we assume that the effective charge for each carbon atom is: $\eta_s \approx 2.4e$. With this assumption, the formula stated above can be used to estimate the concentration of the $\mathcal{B}$-form centers, provided that $\alpha_s(\sigma)$ is set equal to the sum of the absorption coefficients of all six LVM's divided by 2. This factor of 2 reflects the two ''$C_s$ units'' in the $\mathcal{B}$ form. The integral of $\alpha_s(\sigma)$ has been determined from the spectrum recorded after 820-min heat treatment at room temperature and subsequent cooling to 10 K in darkness. Under these conditions, all the $C_s$–$C_i$ centers have the $\mathcal{B}$ configuration and $N = N_{C_s-C_i}$. We find that $N_{C_s-C_i} \approx 4.2 \times 10^{16}$ cm$^{-3}$, which again is very close to the concentration determined from the intensity of the 7819-cm$^{-1}$ line. Hence, also the intensities of the LVM's of the $\mathcal{A}$ and the $\mathcal{B}$ form appear quantitatively consistent with the microscopic models.

## V. CONCLUSIONS

The metastable dicarbon defect $C_s$–$C_i$ in silicon has been studied by IR absorption spectroscopy. A number of carbon-related absorption lines have been observed and identified as LVM's of the $\mathcal{A}$ and $\mathcal{B}$ form of $C_s$–$C_i{}^0$. The observed mode frequencies are in close agreement with those calculated from *ab initio* theory. Moreover, the intensities of the LVM's are consistent with the atomic models of the two configurations, which were suggested previously.

## ACKNOWLEDGMENTS

We thank Lennart Lindström, Linköping University, for providing the $^{13}$C-doped silicon samples and Pia Bomholt for preparing the samples for optical measurements. This work was supported by the Danish National Research Foundation through the Aarhus Center for Atomic Physics. E.V.L. also acknowledges a grant from the Russian Basic Research Foundation (Grant No. 96-02-18077-a).

[1] For a recent review, see G. Davies and R.C. Newman, in *Handbook on Semiconductors*, edited by T.S. Moss (Elsevier Science, Amsterdam, 1994), Vol. 3b, p. 1557, and references therein.
[2] A.R. Bean and R. Newman, Solid State Commun. **8**, 175 (1970).
[3] G.D. Watkins and K.L. Brower, Phys. Rev. Lett. **36**, 1329 (1976).
[4] G.D. Watkins, in *Radiation Effects in Semiconductors*, edited by M. Hulin (Dunod, Paris, 1965).
[5] A.V. Yukhnevich and V.D. Tkachev, Fiz. Tverd. Tela (Leningrad) **8**, 1264 (1966) [Sov. Phys. Solid State **8**, 1004 (1966)].
[6] K.L. Brower, Phys. Rev. B **9**, 2607 (1974).
[7] A.R. Bean, R.C. Newman, and R.S. Smith, J. Phys. Chem. Solids **31**, 739 (1970).
[8] K. Natarajan and E.L. Heasell, Phys. Status Solidi A **28**, 603 (1975).
[9] G.E. Jellison, J. Appl. Phys. **53**, 5715 (1982).
[10] L.W. Song, X.D. Zhan, and G.D. Watkins, Phys. Rev. B **42**, 5765 (1990).
[11] K.P O'Donnell, K.M. Lee, and G.D. Watkins, Physica B&C **116**, 258 (1983).
[12] E.C. Lightowlers and A.N. Safonov, Mater. Sci. Forum **258-263**, 617 (1997).
[13] P. Leary, R. Jones, S. Oberg, and V.J.B. Torres, Phys. Rev. B **55**, 2188 (1997).
[14] P. Leary and R. Jones (private communication).
[15] R.B. Capaz, A. Dal Pino, Jr., and J.D. Joannopoulos, Phys. Rev. B **58**, 9845 (1998).
[16] *Annual Book of ASTM Standards* (ASTM, Philadelphia,1988), Vol. 10.05.
[17] J.W. Corbett, G.D. Watkins, R.M. Chrenko, and R.S. McDonald, Phys. Rev. **121**, 1015 (1961).
[18] J. Menendez and M. Cardona, Phys. Rev. B **29**, 2051 (1984).
[19] S.P. Chapell, M. Claybourn, R.C. Newman, and K.G. Barraclough, Semicond. Sci. Technol. **3**, 1047 (1988).
[20] R.C. Newman, in *Imperfections in III/V Materials, Vol. 38 of Semiconductors and Semimetals*, edited by E.R. Weber (Academic, Boston, 1993), p. 117.
[21] In principle this formula is correct only for three-dimensional LVM's, and for, e.g., a nondegenerate mode a factor of 3 should be included in the denominator on the right side of the equation. However, the effective charges stated in the text were calculated with the three-dimensional expression, and, therefore, this should be used to calculate *N*.
[22] B. Clerjaud and D. Côte, J. Phys.: Condens. Matter **4**, 9919 (1992).